INTERNATIONAL JOURNAL FOR NUMERICAL METHODS IN FLUIDS
Int. J. Numer. Meth. Fluids 2006; **51**:1001–1016
Published online 6 December 2005 in Wiley InterScience (www.interscience.wiley.com). DOI: 10.1002/fld.1128

On a modification of GLS stabilized FEM for solving incompressible viscous flows

P. Burda[1,*,†], J. Novotný[2,‡] and J. Šístek[1,§]

[1]*Department of Mathematics, Czech University of Technology, Karlovo náměstí 13, CZ-121 35 Praha 2, Czech Republic*
[2]*Institute of Thermomechanics, Czech Academy of Science, Dolejškova 5, CZ-182 00 Praha 8, Czech Republic*

SUMMARY

We deal with 2D flows of incompressible viscous fluids with high Reynolds numbers. Galerkin Least Squares technique of stabilization of the finite element method is studied and its modification is described. We present a number of numerical results obtained by the developed method, showing its contribution to solving flows with high Reynolds numbers. Several recommendations and remarks are included. We are interested in positive as well as negative aspects of stabilization, which cannot be divorced. Copyright © 2005 John Wiley & Sons, Ltd.

KEY WORDS: FEM; incompressible flow; stabilization; GLS; semiGLS

1. INTRODUCTION

The idea of stabilizing the FEM is not quite new in comparison to the history of FEM itself. Many researchers have been involved in this area and have already presented many techniques and results. Let us briefly review several publications related to the approach that we present in this paper. Hughes *et al.* [1] presented the stable Petrov–Galerkin formulation of the Stokes problem in 1986. Douglas and Wang [2] introduced another stabilized method for the Stokes problem in 1988. In the same year; Hughes *et al.* [3] presented SUPG and GLS stabilized finite element methods for the advective–diffusive equation. Their ideas were extended to the Navier–Stokes equations and completed by Franca and Frey [4], Franca and

*Correspondence to: P. Burda, Department of Mathematics, Czech University of Technology, Karlovo náměstí 13, CZ-121 35 Praha 2, Czech Republic.
†E-mail: burda@fsik.cvut.cz
‡E-mail: novotny@bivoj.it.cas.cz
§E-mail: sistek@seznam.cz

Contract/grant sponsor: GAAV; contract/grant number: IAA2120201/02
Contract/grant sponsor: State Research Project; contract/grant number: MSM 684 0770010

Received 2 June 2005
Revised 1 September 2005
Accepted 3 September 2005

Hughes [5], Franca and Madureira [6], and Franca *et al.* [7]. In 1991, Tezduyar presented pressure-stabilizing/Petrov–Galerkin (PSPG) method, another stabilization technique for incompressible viscous fluids [8]. Work of Lube and his co-workers (e.g. Reference [9]) can be mentioned as a recent research in the stabilization of the FEM for fluid dynamics.

Mainly the works of Franca and Hughes provide the theoretical basis for the presented research. We modify the Galerkin Least-Squares (GLS) method introduced in Reference [3] and solve flows with markably higher Reynolds numbers than without stabilization. We present several results of numerical experiments which show the impact of this stabilization on the solution and people who use stabilization techniques should be aware of it.

2. MODEL PROBLEM

Let Ω be an open bounded domain in $\mathbb{R}^2$ filled with an incompressible viscous fluid, and let Γ be its boundary. Isothermal flow of such fluid is governed by the following Navier–Stokes system of partial differential equations (nonconservative form)

- *Unsteady flow*

$$\frac{\partial \mathbf{u}}{\partial t} + (\mathbf{u}\cdot\nabla)\mathbf{u} - \nu\Delta\mathbf{u} + \nabla p = \mathbf{f} \quad \text{in } \Omega\times[0,T] \tag{1}$$

$$\nabla\cdot\mathbf{u} = 0 \quad \text{in } \Omega\times[0,T] \tag{2}$$

$$\mathbf{u} = \mathbf{g} \quad \text{on } \Gamma_g\times[0,T] \tag{3}$$

$$-\nu(\nabla\mathbf{u})\mathbf{n} + p\mathbf{n} = \mathbf{0} \quad \text{on } \Gamma_h\times[0,T] \tag{4}$$

$$\mathbf{u} = \mathbf{u}_0 \quad \text{in } \Omega,\ t=0 \tag{5}$$

- *Steady flow*

$$(\mathbf{u}\cdot\nabla)\mathbf{u} - \nu\Delta\mathbf{u} + \nabla p = \mathbf{f} \quad \text{in } \Omega \tag{6}$$

$$\nabla\cdot\mathbf{u} = 0 \quad \text{in } \Omega \tag{7}$$

$$\mathbf{u} = \mathbf{g} \quad \text{on } \Gamma_g \tag{8}$$

$$-\nu(\nabla\mathbf{u})\mathbf{n} + p\mathbf{n} = \mathbf{0} \quad \text{on } \Gamma_h \tag{9}$$

where

- t denotes time variable,
- $\mathbf{u} = (u_1, u_2)^{\mathrm{T}}$ denotes the vector of flow velocity,
- p denotes the pressure divided by the density,
- ν denotes the kinematic viscosity of the fluid supposed to be constant,
- $\mathbf{f}$ denotes the density of volume forces per mass unit,
- Γ_g and Γ_h are two subsets of Γ satisfying $\bar{\Gamma} = \bar{\Gamma}_g \cup \bar{\Gamma}_h$, $\mu_{\mathbb{R}^1}(\Gamma_g \cap \Gamma_h) = 0$,
- $\mathbf{n}$ denotes an outer normal vector to the boundary Γ with unit length,
- $\mathbf{g}$ is a given function satisfying $\int_\Gamma \mathbf{g}\cdot\mathbf{n}\,\mathrm{d}\Gamma = 0$ in the case of $\Gamma = \Gamma_g$,
- $\mathbf{u}_0$ is a given flow field satisfying $\nabla\cdot\mathbf{u}_0 = 0$.

3. APPROXIMATION OF THE PROBLEM BY FEM

First we derive the weak formulation of the Navier–Stokes equations (1)–(5) in the manner of mixed methods, i.e. usage of different function spaces of test functions for the momentum equation and for the continuity equation (cf. Reference [10]). Let us define vector function spaces V_g and V by

$$V_g = \{\mathbf{v} = (v_1, v_2)^{\mathrm{T}} \mid \mathbf{v} \in [H^1(\Omega)]^2; \mathbf{Tr}\ v_i = g_i, i = 1, 2\}$$

$$V = \{\mathbf{v} = (v_1, v_2)^{\mathrm{T}} \mid \mathbf{v} \in [H_0^1(\Omega)]^2\}$$

where $H^1(\Omega)$ and $H_0^1(\Omega)$ are the usual Sobolev spaces. Let additionally $L_2(\Omega)$ be the space of square integrable functions on Ω, and let $L_2(\Omega)/\mathbb{R}$ be the space of functions in $L_2(\Omega)$ ignoring an additive constant.

Then the *weak unsteady Navier–Stokes problem* consists of finding $\mathbf{u}(t) = (u_1(t), u_2(t))^{\mathrm{T}} \in V_g$ and $p(t) \in L_2(\Omega)/\mathbb{R}$ satisfying for any $t \in [0, T]$

$$\int_\Omega \frac{\partial \mathbf{u}}{\partial t} \cdot \mathbf{v}\, \mathrm{d}\Omega + \int_\Omega (\mathbf{u} \cdot \nabla)\mathbf{u} \cdot \mathbf{v}\, \mathrm{d}\Omega + \nu \int_\Omega \nabla \mathbf{u} : \nabla \mathbf{v}\, \mathrm{d}\Omega - \int_\Omega p \nabla \cdot \mathbf{v}\, \mathrm{d}\Omega = \int_\Omega \mathbf{f} \cdot \mathbf{v}\, \mathrm{d}\Omega \tag{10}$$

$$\int_\Omega \psi \nabla \cdot \mathbf{u}\, \mathrm{d}\Omega = 0 \tag{11}$$

$$\mathbf{u} - \mathbf{u}_g \in V \tag{12}$$

for all $\mathbf{v} \in V$ and $\psi \in L^2(\Omega)$, where $\mathbf{u}_g \in V_g$ is a representation of the Dirichlet boundary condition $\mathbf{g}$ in (3). We denote

$$\nabla \mathbf{u} : \nabla \mathbf{v} = \frac{\partial u_1}{\partial x_1}\frac{\partial v_1}{\partial x_1} + \frac{\partial u_1}{\partial x_2}\frac{\partial v_1}{\partial x_2} + \frac{\partial u_2}{\partial x_1}\frac{\partial v_2}{\partial x_1} + \frac{\partial u_2}{\partial x_2}\frac{\partial v_2}{\partial x_2}$$

For the steady problem (6)–(9), we obtain similar formulation as (10)–(12) without the term with the time derivative in (10) and dependence on time.

Let us divide the domain Ω into N elements T_K of a triangulation $\mathcal{T}_h$ of shape regular family, such that $\bigcup_{K=1}^{N} \bar{T}_K = \bar{\Omega}$, $\mu_{\mathbb{R}^2}(T_K \cap T_L) = 0$, $K \neq L$. Let h_K mean the largest distance in element T_K.

In what follows, we consider Hood–Taylor finite elements P_2P_1 and/or Q_2Q_1, which satisfy Babuška–Brezzi stability condition (*inf–sup* condition) (cf. Reference [11]). Their application leads to the final approximation on the domain Ω satisfying $\mathbf{u}_h \in V_{gh}$ and $p_h \in Q_h$ where

$$V_{gh} = \{\mathbf{v}_h = (v_{h_1}, v_{h_2})^{\mathrm{T}} \in [\mathscr{C}(\bar{\Omega})]^2;\ v_{h_i}|_{T_K} \in R_2(\overline{T_K}),\ K = 1, \ldots, N,\ i = 1, 2,\ \mathbf{v}_h = \mathbf{g}$$

in nodes on $\Gamma_g\}$

$$Q_h = \{\psi_h \in \mathscr{C}(\bar{\Omega});\ \psi_h|_{T_K} \in R_1(\overline{T_K}),\ K = 1, \ldots, N\}$$

where

$$R_m(\overline{T_K}) = \begin{cases} P_m(\overline{T_K}) & \text{if } T_K \text{ is a triangle} \\ Q_m(\overline{T_K}) & \text{if } T_K \text{ is a quadrilateral} \end{cases}$$

and $\mathscr{C}(\bar{\Omega})$ denotes the space of continuous functions on $\bar{\Omega}$. Additionally, we introduce the space

$$V_h = \{\mathbf{v}_h = (v_{h_1}, v_{h_2})^{\mathrm{T}} \in [\mathscr{C}(\bar{\Omega})]^2;\ v_{h_i}|_{T_K} \in R_2(\overline{T_K}),\ K = 1, \ldots, N,\ i = 1, 2,\ \mathbf{v}_h = \mathbf{0} \text{ in nodes on } \Gamma_g\}$$

Since these function spaces satisfy $V_{gh} \subset V_g$, $V_h \subset V$, and $Q_h \subset L_2(\Omega)/\mathbb{R}$, we can introduce *semidiscrete unsteady Navier–Stokes problem*:

Find $\mathbf{u}_h(t) \in V_{gh}$, $t \in [0, T]$ and $p_h(t) \in Q_h$, $t \in [0, T]$ satisfying for any $t \in [0, T]$

$$\int_\Omega \frac{\partial \mathbf{u}_h}{\partial t} \cdot \mathbf{v}_h \, \mathrm{d}\Omega + \int_\Omega (\mathbf{u}_h \cdot \nabla)\mathbf{u}_h \cdot \mathbf{v}_h \, \mathrm{d}\Omega + \nu \int_\Omega \nabla \mathbf{u}_h : \nabla \mathbf{v}_h \, \mathrm{d}\Omega$$

$$- \int_\Omega p_h \nabla \cdot \mathbf{v}_h \, \mathrm{d}\Omega = \int_\Omega \mathbf{f} \cdot \mathbf{v}_h \, \mathrm{d}\Omega, \quad \forall \mathbf{v}_h \in V_h \tag{13}$$

$$\int_\Omega \psi_h \nabla \cdot \mathbf{u}_h \, \mathrm{d}\Omega = 0, \quad \forall \psi_h \in Q_h \tag{14}$$

$$\mathbf{u}_h - \mathbf{u}_{gh} \in V_h \tag{15}$$

4. STABILIZED FORMULATION

Following ideas of Hughes and Franca [3, 6], we apply the GLS stabilizing technique with two modifications:

1. Stabilization of the continuity equation is not considered. For this reason, we call the technique *semiGLS* (abbreviated sGLS). Since most problems are caused by the advective term, we find stabilization of it as most important. We performed several experiments with stabilization of the continuity equation applied, but the results were disastrous.
2. The algorithm is derived for the Navier–Stokes equations with Laplacian in the diffusive term instead of whole symmetric part of the velocity gradient. This formulation makes the derivations much simpler, therefore less mistakes can be made and stay undetected.

Applying stabilization to the momentum equation (13) and adding the continuity equation (14), we introduce the stabilized problem:

Find $\mathbf{u}_h(t) \in V_{gh}$, $t \in [0, T]$ and $p_h(t) \in Q_h$, $t \in [0, T]$ satisfying for any $t \in [0, T]$

$$B_{\mathrm{sGLS}}(\mathbf{u}_h, p_h; \mathbf{v}_h, \psi_h) = L_{\mathrm{sGLS}}(\mathbf{v}_h, \psi_h), \quad \forall \mathbf{v}_h \in V_h,\ \forall \psi_h \in Q_h \tag{16}$$

$$\mathbf{u}_h - \mathbf{u}_{gh} \in V_h \tag{17}$$

where

$$B_{\mathrm{sGLS}}(\mathbf{u}_h, p_h; \mathbf{v}_h, \psi_h) \equiv \int_\Omega \frac{\partial \mathbf{u}_h}{\partial t} \cdot \mathbf{v}_h \, \mathrm{d}\Omega + \int_\Omega (\mathbf{u}_h \cdot \nabla)\mathbf{u}_h \cdot \mathbf{v}_h \, \mathrm{d}\Omega$$
$$+ \nu \int_\Omega \nabla \mathbf{u}_h : \nabla \mathbf{v}_h \, \mathrm{d}\Omega - \int_\Omega p_h \nabla \cdot \mathbf{v}_h \, \mathrm{d}\Omega + \int_\Omega \psi_h \nabla \cdot \mathbf{u}_h \, \mathrm{d}\Omega$$
$$+ \sum_{K=1}^{N} \int_{T_K} \left[\frac{\partial \mathbf{u}_h}{\partial t} + (\mathbf{u}_h \cdot \nabla)\mathbf{u}_h - \nu \Delta \mathbf{u}_h + \nabla p_h \right]$$
$$\cdot \tau \left[(\mathbf{u}_h \cdot \nabla)\mathbf{v}_h - \nu \Delta \mathbf{v}_h + \nabla \psi_h \right] \mathrm{d}\Omega$$
$$L_{\mathrm{sGLS}}(\mathbf{v}_h, \psi_h) \equiv \int_\Omega \mathbf{f} \cdot \mathbf{v}_h \, \mathrm{d}\Omega + \sum_{K=1}^{N} \int_{T_K} \mathbf{f} \cdot \tau [(\mathbf{u}_h \cdot \nabla)\mathbf{v}_h - \nu \Delta \mathbf{v}_h + \nabla \psi_h] \, \mathrm{d}\Omega$$

Here τ is positive stabilization parameter. Modifying formulas from Reference [6], we compute it as

$$\tau = \frac{\xi(Re_K(\mathbf{x}))}{\sqrt{\lambda_K} |\mathbf{u}(\mathbf{x})|_2} \tag{18}$$

where

$$Re_K(\mathbf{x}) = \frac{|\mathbf{u}(\mathbf{x})|_2}{4\sqrt{\lambda_K}\nu}$$
$$\xi(Re_K(\mathbf{x})) = \begin{cases} Re_K(\mathbf{x}), & 0 \leqslant Re_K(\mathbf{x}) < 1 \\ 1, & Re_K(\mathbf{x}) \geqslant 1 \end{cases}$$
$$\lambda_K = \max_{0 \neq \mathbf{v} \in (R_2(T_K)/\mathbb{R})^2} \frac{\|\Delta \mathbf{v}\|^2_{0,T_K}}{\|\nabla \mathbf{v}\|^2_{0,T_K}}$$
$$|\mathbf{u}(\mathbf{x})|_2 = \left(\sum_{i=1}^{2} |u_i(\mathbf{x})|^2 \right)^{1/2}$$

Parameter λ_K is computed for each element as the largest eigenvalue of the problem

$$(\Delta \mathbf{w}, \Delta \mathbf{v}) = \lambda_K (\nabla \mathbf{w}, \nabla \mathbf{v}) \quad \forall \mathbf{v} \in (R_2(T_K)/\mathbb{R})^2 \tag{19}$$

This is done once, before entering the main computational loop of the Newton method, since λ_K is not a function of velocity and depends only on the computational mesh through space functions on element K.

Stabilized formulation for the steady problem (6)–(9) is derived analogously and is simpler.

Let us investigate the dependence of τ on local Reynolds number $Re_K(\mathbf{x})$ given by (18). We can observe that $Re_K(\mathbf{x})$ is a linear function of $|\mathbf{u}(\mathbf{x})|_2$ for constant viscosity on element K, i.e.

$$Re_K(\mathbf{x}) = C_1 |\mathbf{u}(\mathbf{x})|_2 \tag{20}$$

where $C_1 = 1/(4\sqrt{\lambda_K}\nu)$.

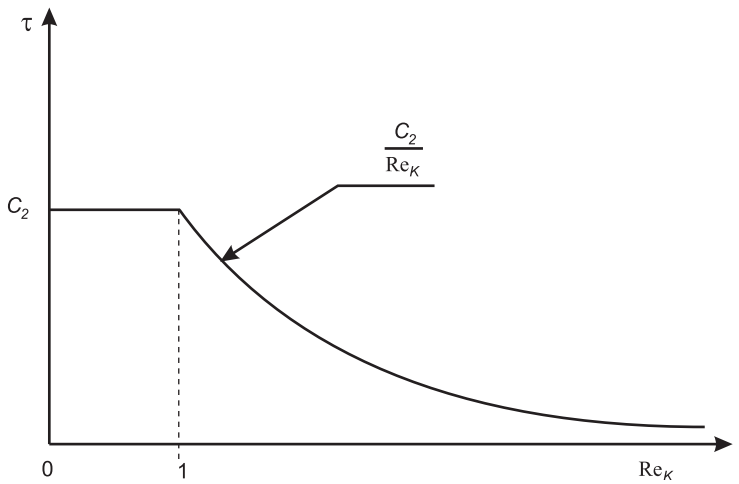

Figure 1. Plot of $\tau(Re_K)$.

Substituting (20) in (18) we get

$$\tau(Re_K(\mathbf{x}),\mathbf{x}) = \begin{cases} C_2, & 0 \leqslant Re_K(\mathbf{x}) < 1 \\ \dfrac{C_3}{|\mathbf{u}(\mathbf{x})|_2} = \dfrac{C_2}{Re_K(\mathbf{x})}, & Re_K(\mathbf{x}) \geqslant 1 \end{cases}$$

where $C_2 = 1/(4\lambda_K \nu)$ and $C_3 = 1/\sqrt{\lambda_K}$, cf. Figure 1.

5. IMPLEMENTATION OF THE METHOD

In our implementation, we employ the implicit Euler method (also known as the backward difference method) for time discretization of the problem (16)–(17), i.e. time derivative is substituted as

$$\frac{\partial \mathbf{u}_h}{\partial t} \approx \frac{\mathbf{u}_h^{n+1} - \mathbf{u}_h^n}{\vartheta}$$

where ϑ denotes a constant time step. This leads to fully implicit method for finding $\mathbf{u}_h$ in $(n+1)$th time layer. Resulting system of nonlinear equations is solved by the Newton method in each time layer, employing direct solver for solving the linearized system in each iteration.

6. NUMERICAL EXPERIMENTS

The method was tested on several problems for verification and to review its behaviour. Results obtained by the algorithm are marked as *semiGLS* algorithm results.

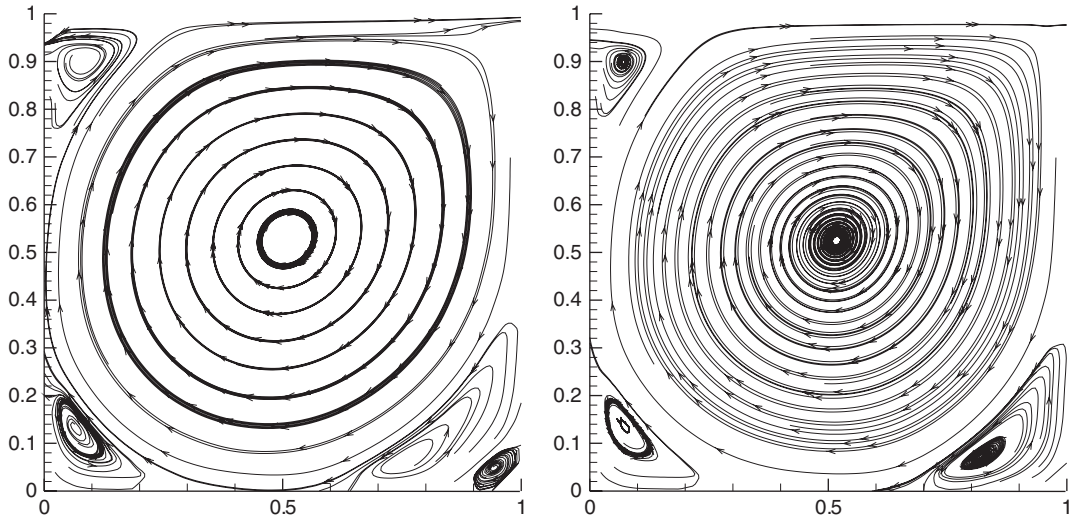

Figure 2. Streamlines by the Newton method without stabilization (left) and by the semiGLS algorithm (right), $Re = 10\,000$, mesh 32×32.

6.1. Steady solution of lid driven cavity

Popular benchmark problem for testing numerical schemes is the 'lid driven cavity'. Computational domain is of square shape with unit length of side. Dirichlet boundary conditions are prescribed on the boundary: value of horizontal velocity is prescribed on the upper side, zero boundary conditions on the rest of the boundary representing a wall.

Many solutions of this problem were presented by various authors. Here are some representatives: in Reference [12], solutions for Reynolds numbers 1000, 3200, and 5000 obtained on nonuniform grid of approximately 8800 elements are presented; in Reference [9], result for Reynolds number 7500 on quasi-uniform mesh of 96×96 elements is presented; solutions for Reynolds number 10 000 obtained by several methods on the mesh of 64×64 elements are published in Reference [13], and in Reference [7], outstanding results for Reynolds number 500 000 on the mesh of 30×30 elements are presented.

Solution by the developed algorithm was performed on three uniform meshes of quadrilateral elements—of 32×32 (1024) elements, of 64×64 (4096) elements, and of 128×128 (16 384) elements.

To observe the effect of stabilization, solutions obtained by the Newton method without stabilization together with solutions computed by the semiGLS algorithm for Reynolds number 10 000 on all three meshes are presented in Figures 2–4. Moreover, we can review the sensitivity to the fineness of the computational mesh in these figures.

We can observe, that streamlines are not encircled for the GLS method showing the loss of accuracy induced by the stabilization. This defect is decreasing with refining of the mesh.

We evaluate the effect of stabilization as the difference of solutions obtained with and without stabilization by

$$\delta_\eta = \sqrt{\frac{\sum_{i=1}^{n} (\eta_{\mathrm{sGLS}_i} - \eta_{\mathrm{Newton}_i})^2}{\sum_{i=1}^{n} \eta_{\mathrm{Newton}_i}^2}} \times 100\ (\%) \tag{21}$$

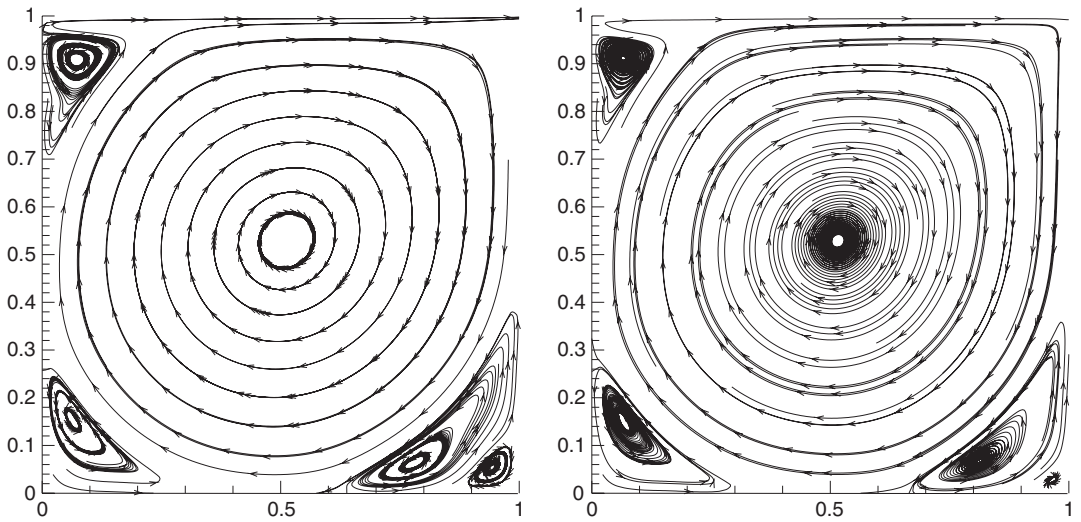

Figure 3. Streamlines by the Newton method without stabilization (left) and by the semiGLS algorithm (right), $Re = 10\,000$, mesh 64×64.

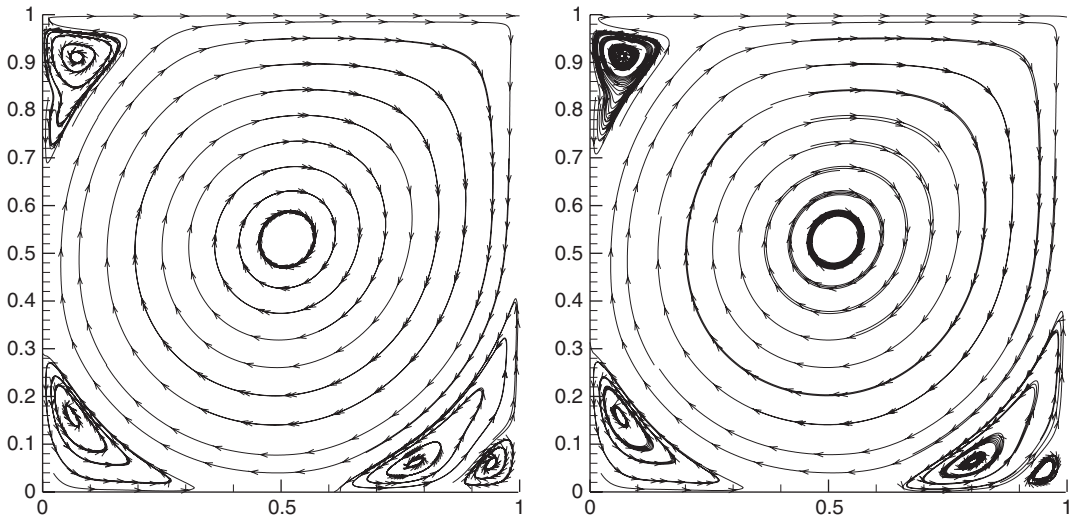

Figure 4. Streamlines by the Newton method without stabilization (left) and by the semiGLS algorithm (right), $Re = 10\,000$, mesh 128×128.

where η represents in turn u_{h1}, u_{h2} and p_h, n denotes number of nodes with η given, η_{sGLS} denotes the solution obtained by the semiGLS algorithm and η_{Newton} denotes the solution obtained by the Newton method without stabilization. Results are summarized in Table I.

Table I. Differences between solutions obtained with and without stabilization.

Mesh	32×32	64×64	128×128
$\delta_{u_{h1}}$ (%)	41.69	39.07	21.42
$\delta_{u_{h2}}$ (%)	70.81	49.12	22.24
δ_{p_h} (%)	197.90	137.10	42.82

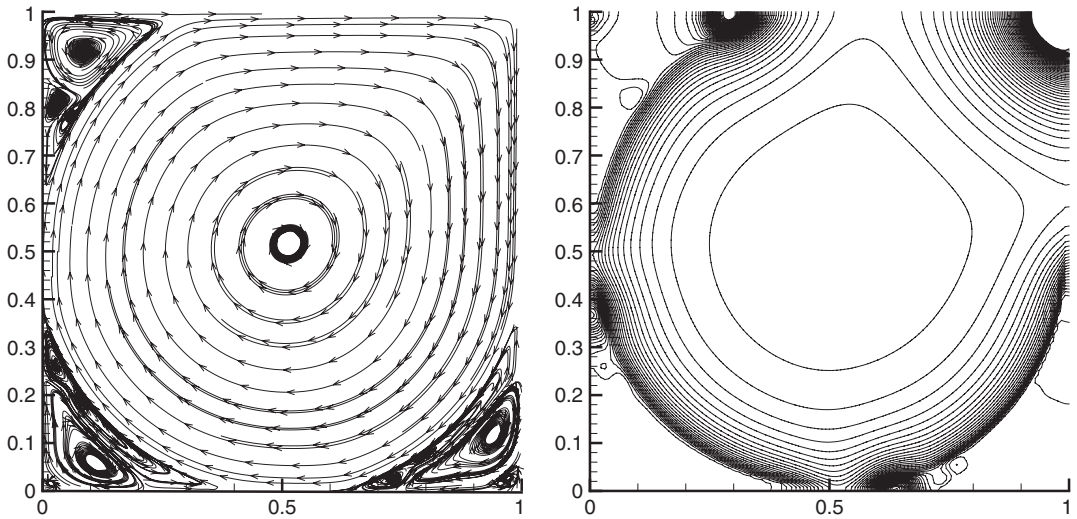

Figure 5. Streamlines (left) and pressure contours (right) by the semiGLS algorithm on the mesh 128×128, $Re = 100\,000$.

Differences of solutions obtained by the semiGLS method from those obtained by the Newton method computed by (21) are big for the problem of cavity.

To extend results to higher Reynolds numbers, solution for $Re = 100\,000$ on the mesh 128×128 is presented in Figure 5.

Although the continuation method was applied to achieve higher Reynolds numbers, we detected limits of convergence of the Newton method for all three meshes. We observed, that on the mesh 32×32, we were not able to get results above $Re \approx 28\,000$, on the mesh 64×64 above $Re \approx 50\,000$, and on the mesh 128×128 above $Re \approx 120\,000$. For comparison, such limit was around $Re \approx 12\,500$ on the mesh 32×32 for the method without stabilization ($\tau = 0$).

Another interesting effect was observed during the computations. Since it is known that stabilized methods are in general, sensitive to stabilization parameters, we tried to modify the computed parameter τ by a quotient 0.7–1.5. This improved the convergence, and we were able to reach higher Reynolds numbers, e.g. $Re = 70\,000$ on the mesh 64×64 elements.

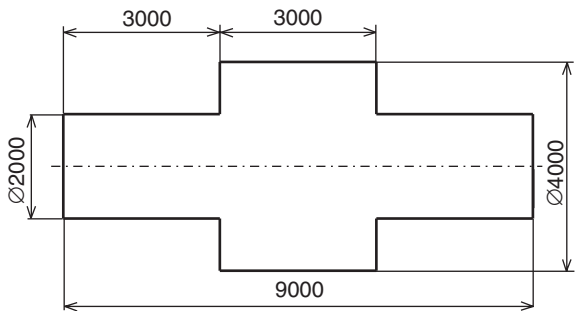

Figure 6. Geometry of the channel.

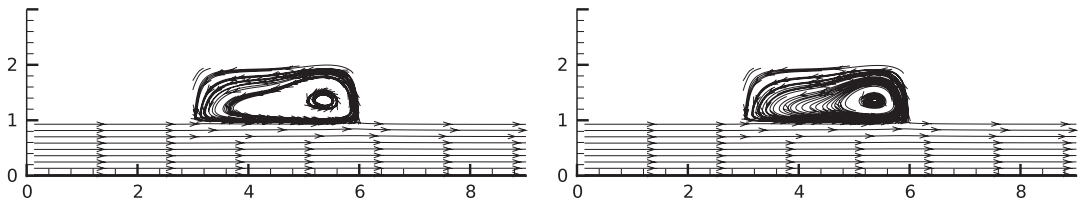

Figure 7. Streamlines in the channel by the Newton method without stabilization (left) and streamlines by the semiGLS algorithm (right), $Re = 1000$.

Table II. Differences between solutions obtained with and without stabilization.

Mesh	Channel (Figure 6)
$\delta_{u_{h1}}$ (%)	0.0718
$\delta_{u_{h2}}$ (%)	2.7202
δ_{p_h} (%)	0.5139

6.2. Steady solution of flow in channel with sudden extension of diameter

Steady flow in 2D channel with abruptly extended diameter (Figure 6) is another testing problem. This problem is complicated due to singularities of solution in the vicinity of non-convex internal corners. The aspect of suitable mesh generation for such problems is studied in References [14, 15]. We compare solutions with and without semiGLS stabilization in this paper. Streamlines are presented in Figure 7 for Reynolds number 1000. For the symmetry of the problem, solution is found only on the upper half of the section. Differences between solutions computed by (21) are listed in Table II. Parabolic horizontal velocity distribution is prescribed on the inflow (left) part of the boundary, 'do nothing' condition is considered on the outflow (right) part of it, zero velocity is prescribed on the upper part of the boundary representing wall with 'no slip' and symmetry is considered on the lower part of it (see Reference [15] for details).

Additionally, we present streamlines, plots of velocities and pressure for Reynolds number 80 000 in Figures 8 and 9.

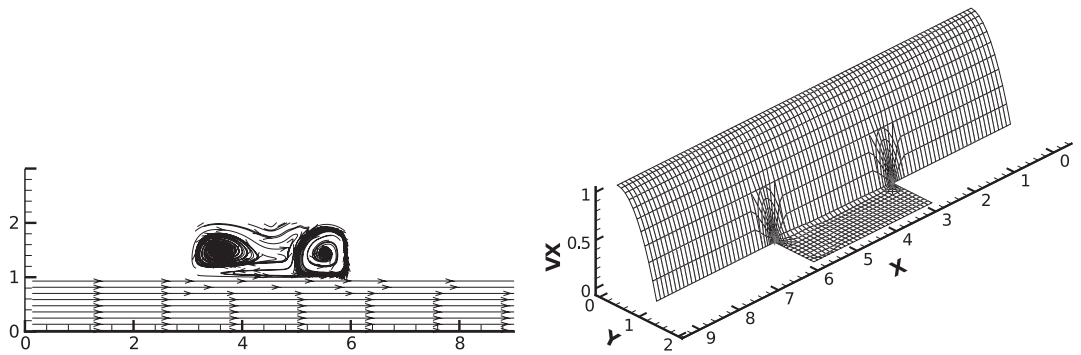

Figure 8. Streamlines (left) and plot of velocity u_{h1} (right) by the semiGLS algorithm, $Re = 80\,000$.

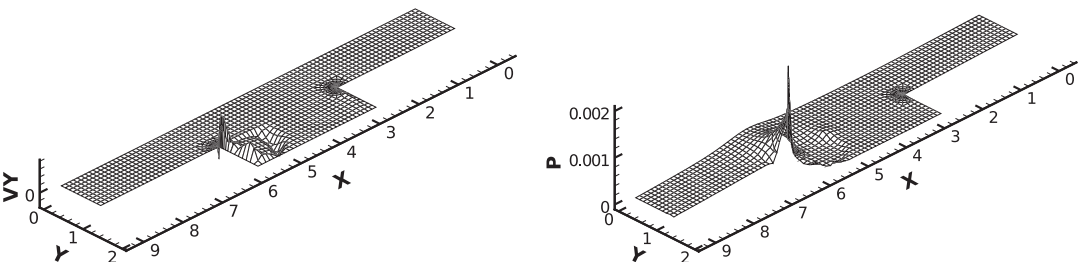

Figure 9. Plot of velocity u_{h2} (left) and pressure (right) by the semiGLS algorithm, $Re = 80\,000$.

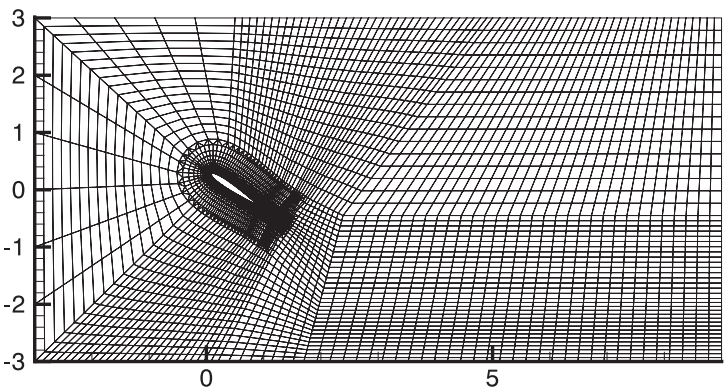

Figure 10. Computational mesh for NACA 0012 problem, angle of incidence of 34°.

6.3. *Unsteady solution of flow past NACA 0012 airfoil*

Unsteady flow past NACA 0012 airfoil was investigated as a more practical application. Results of this problem for angle of incidence of 34° and Reynolds number 1000 obtained by the unconditionaly stable projection FEM were presented by Guermond and Quartapelle in

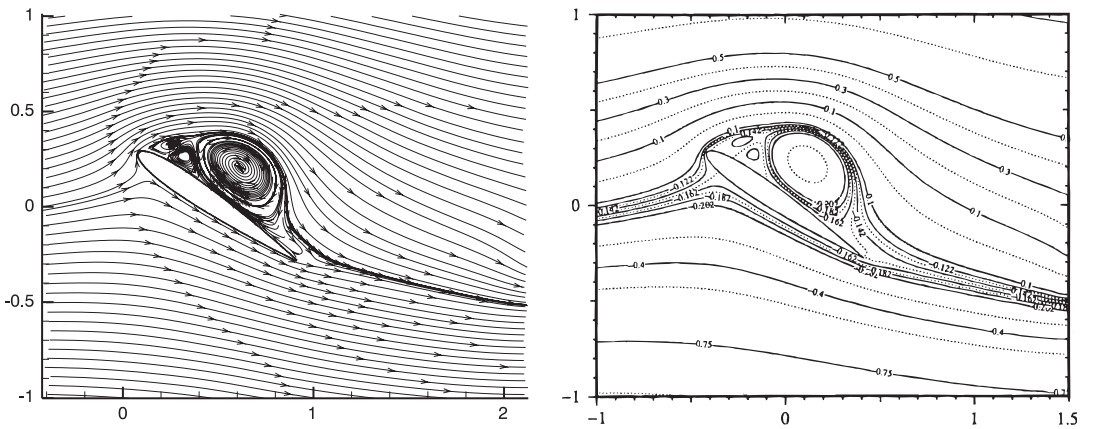

Figure 11. Streamlines by the semiGLS algorithm (left) and by Guermond and Quartapelle [12] (right), $t = 1.6$ s, $Re = 1000$.

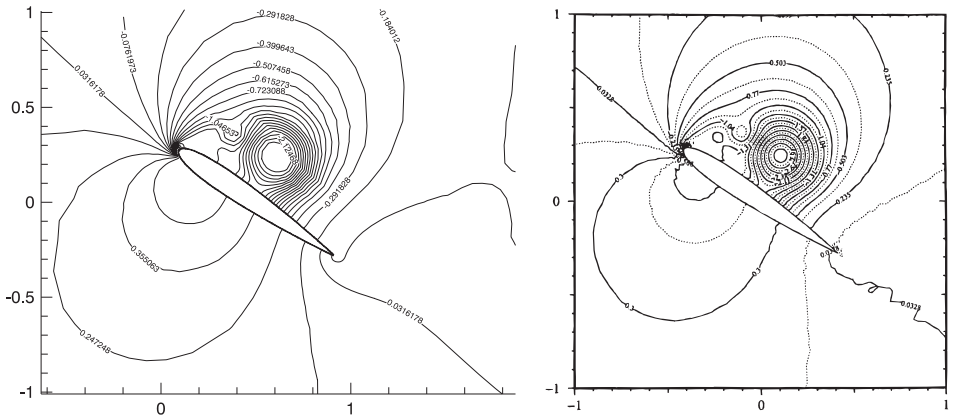

Figure 12. Pressure contours by the semiGLS algorithm (left) and by Guermond and Quartapelle [12] (right), $t = 1.6$ s, $Re = 1000$.

Reference [12]. In Figures 11–15, these results are compared to ours obtained by the semiGLS algorithm. Streamlines and pressure contours for the problem with Reynolds number 100 000 in several time layers are presented in Figures 16–19. The computational mesh is shown in Figure 10. It contains 6220 elements, 18 478 nodes, and 43 085 degrees of freedom. We consider zero initial condition, unit horizontal velocity on the left part of the boundary and 'do nothing' boundary condition on the rest of it. Time step sizes for simulation for Reynolds number 1000 are 0.01 s and for Reynolds number 100 000 are 0.005 s (see Reference [15] for details).

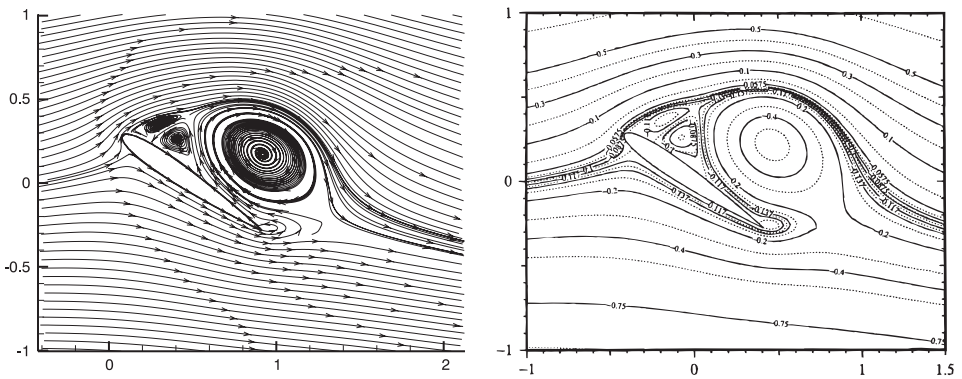

Figure 13. Streamlines by the semiGLS algorithm (left) and by Guermond and Quartapelle [12] (right), $t = 2.6\,\mathrm{s}$, $Re = 1000$.

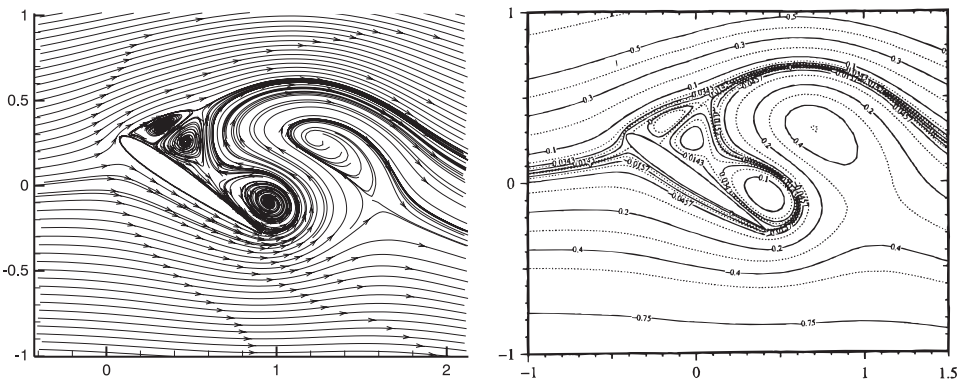

Figure 14. Streamlines by the semiGLS algorithm (left) and by Guermond and Quartapelle [12] (right), $t = 3.6\,\mathrm{s}$, $Re = 1000$.

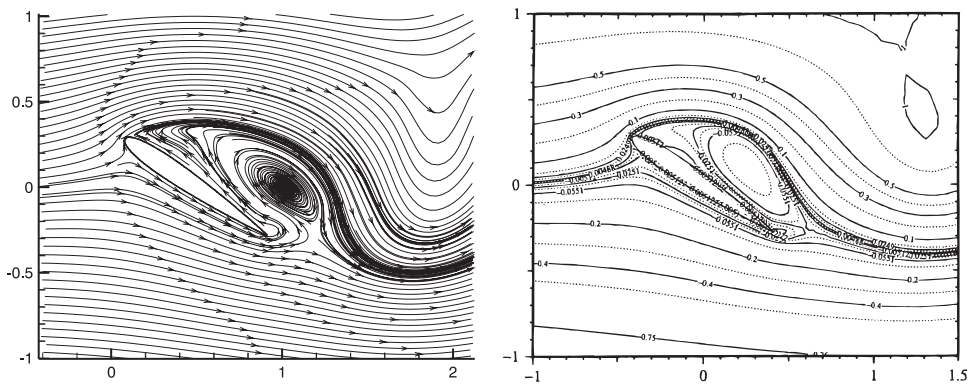

Figure 15. Streamlines by the semiGLS algorithm (left) and by Guermond and Quartapelle [12] (right), $t = 6.0\,\mathrm{s}$, $Re = 1000$.

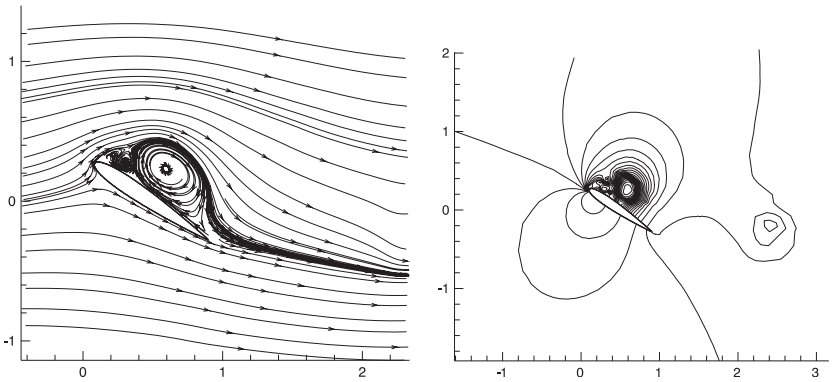

Figure 16. Streamlines (left) and pressure contours (right) by the semiGLS algorithm, $t = 1.6$ s, $Re = 100\,000$.

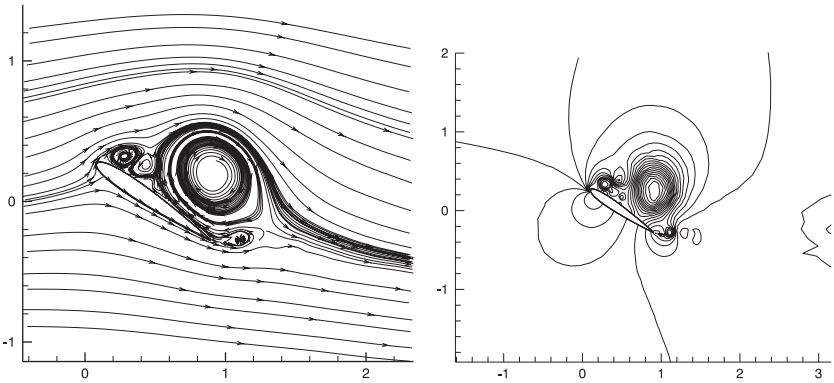

Figure 17. Streamlines (left) and pressure contours (right) by the semiGLS algorithm, $t = 2.6$ s, $Re = 100\,000$.

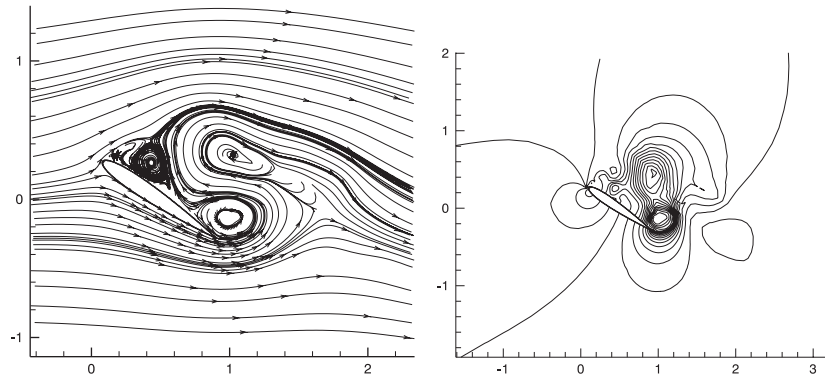

Figure 18. Streamlines (left) and pressure contours (right) by the semiGLS algorithm, $t = 3.6$ s, $Re = 100\,000$.

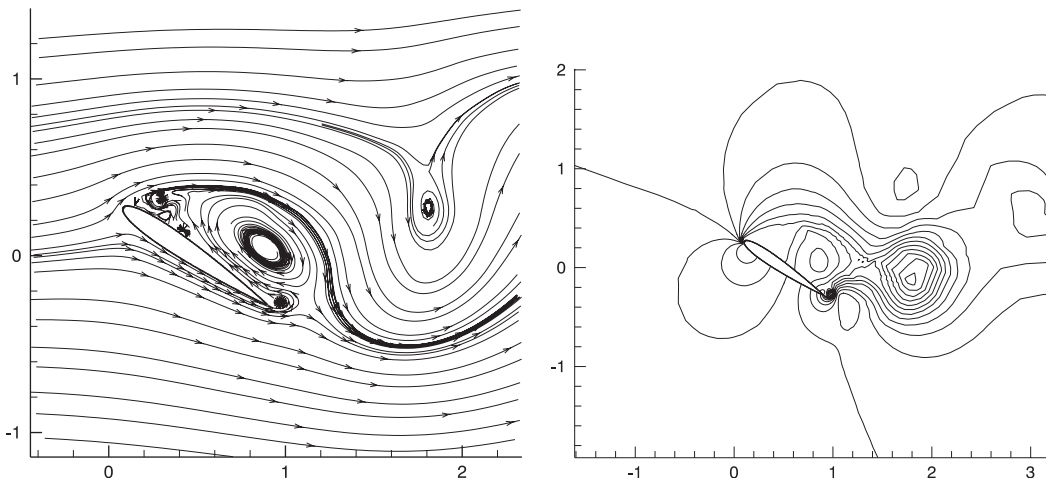

Figure 19. Streamlines (left) and pressure contours (right) by the semiGLS algorithm, $t = 6.0\,\mathrm{s}$, $Re = 100\,000$.

7. CONCLUSION

The motivation for using stabilization techniques comes from the desire of solving problems for higher Reynolds numbers.

We achieved our main goal—to develop an applicable algorithm based on the FEM equipped with stabilization. The algorithm has been verified by several numerical experiments and performed contributive results. More about the algorithm and other numerical results can be found in Reference [15].

On the problem of cavity for $Re = 10\,000$ we show, that applying stabilization induces loss of accuracy. Distortion of solution could be significant for some problems (Figures 2–4 and Table I), but could also play negligible role for other problems (Figure 7 and Table II).

It was observed that presented stabilization technique leads to improvement of stability of the Newton method to approximately 'double' Reynolds number. Similar effect was observed for the refinement of the computational mesh with half element size.

This results in recommendation, that for solving flows for higher Reynolds numbers, applying of stabilization techniques should be efficiently combined with a suitable refinement. Stabilization should be applied carefully and reliable tool for error estimation for semiGLS technique is still desired.

REFERENCES

1. Hughes TJR, Franca LP, Balestra M. A new finite element formulation for computational fluid dynamics: V. Circumventing the Babuška–Brezzi condition: a stable Petrov–Galerkin formulation of the Stokes problem accommodating equal-order interpolations. *Computer Methods in Applied Mechanics and Engineering* 1986; **59**:85–99.
2. Douglas Jr J, Wang J. An absolutely stabilized finite element method for the Stokes problem. *Mathematics of Computation* 1989; **52**:495–508.

3. Hughes TJR, Franca LP, Hulbert GM. A new finite element formulation for computational fluid dynamics: VIII. The Galerkin/least-squares method for advective–diffusive equations. *Computer Methods in Applied Mechanics and Engineering* 1989; **73**:173–189.
4. Franca LP, Frey SL. Stabilized finite element methods: II. The incompressible Navier–Stokes equations. *Computer Methods in Applied Mechanics and Engineering* 1992; **99**:209–233.
5. Franca LP, Hughes TJR. Convergence analyses of Galerkin least-squares methods for symmetric advective–diffusive forms of the Stokes and incompressible Navier–Stokes equations. *Computer Methods in Applied Mechanics and Engineering* 1993; **105**:285–298.
6. Franca LP, Madureira AL. Element diameter free stability parameters for stabilized methods applied to fluids. *Computer Methods in Applied Mechanics and Engineering* 1993; **105**:395–403.
7. Franca LP, Frey SL, Madureira AL. Two- and three-dimensional simulations of the incompressible Navier–Stokes equations based on stabilized methods. *Computational Fluid Dynamics '94*. Wiley: New York, 1994; 121–128.
8. Tezduyar TE. Stabilized finite element formulations for incompressible flow computations. *Advances in Applied Mechanics* 1991; **28**:1–44.
9. Gelhard T, Lube G, Olshanskii MA, Starcke JH. Stabilized finite element schemes with LBB-stable elements for incompressible flows, preprint, 2004.
10. Girault V, Raviart PG. *Finite Element Method for Navier–Stokes Equations*. Springer: Berlin, 1986.
11. Brezzi F, Fortin M. *Mixed and Hybrid Finite Element Methods*. Springer: Berlin, 1991.
12. Guermond JL, Quartapelle L. Calculation of viscous incompressible viscous flow by an unconditionally stable projection FEM. *Journal of Computational Physics* 1997; **132**:12–33.
13. Turek S. *Efficient Solvers for Incompressible Flow Problems*. Springer: Berlin, 1999.
14. Burda P, Novotný J, Šístek J. Precise FEM solution of a corner singularity using an adjusted mesh. *International Journal for Numerical Methods in Fluids* 2005; **47**(2005):1285–1292.
15. Šístek J. Stabilization of finite element method for solving incompressible viscous flows. *Diploma Thesis*, ČVUT, Praha, 2004.

